Carboxy and Phosphate Esters Cleavage with Mono- and Dinuclear Zinc(II) Macrocyclic Complexes in Aqueous Solution. Crystal Structure of $[Zn_2L1(\mu\text{-}PP)_2(MeOH)_2](ClO_4)_2$ (L1 = [30]aneN$_6$O$_4$, PP$^-$ = Diphenyl Phosphate)

Carla Bazzicalupi,[†] Andrea Bencini,*[,†] Antonio Bianchi,*[,†] Vieri Fusi,[‡] Claudia Giorgi,[†] Piero Paoletti,*[,†] Barbara Valtancoli,[†] and Daniela Zanchi[†]

Department of Chemistry, University of Florence, Via Maragliano 75/77, 50144 Florence, Italy, and Institute of Chemical Sciences, Piazza Rinascimento 6, University of Urbino, Italy

Received December 26, 1996[⊗]

The ligand [30]aneN$_6$O$_4$ (L1) binds two Zn(II) in aqueous solution. The stability constants of the **L1** complexes have been determined at 308.1 K by means of potentiometric measurements. Dinuclear monohydroxo $[Zn_2\mathbf{L1}OH]^{3+}$ and dihydroxo $[Zn_2\mathbf{L1}(OH)_2]^{2+}$ complexes are formed in aqueous solution from neutral to alkaline pH. The kinetics of promoted hydrolysis of *p*-nitrophenyl acetate (NA) was studied. Both hydroxo species promote *p*-nitrophenyl acetate (NA) hydrolysis at 298.1 K with second-order kinetics. The activity of these species in NA hydrolysis is similar to that found for the mononuclear **L2**−Zn-OH$^+$ complex (**L2** = [15]aneN$_3$O$_2$), indicating that the hydrolytic process takes place *via* a simple bimolecular mechanism. The hydrolysis rate of bis(*p*-nitrophenyl) phosphate (BNP) was measured in aqueous solution at 308.1 K in the presence of the **L1** and **L2** zinc complexes. The hydrolysis rate of BNP is increased almost 10-fold by the dinuclear $[Zn_2\mathbf{L1}(OH)_2]^{2+}$ complex with respect to the mononuclear **L2**−Zn-OH$^+$ one. This result indicates a cooperative role of the two metals in the hydrolytic mechanism. A bridging coordination of the phosphate ester to the two Zn(II) ions can be suggested. The crystal structure of $[Zn_2\mathbf{L1}(\mu\text{-}PP)_2(MeOH)_2](ClO_4)_2$ (PP$^-$ = diphenyl phosphate) (space group $P\bar{1}$, a = 10.681(5) Å, b = 12.042(1) Å, c = 13.191(3) Å, α = 74.63(2)°, β = 71.74(3)°, γ = 68.41(2)°, V = 1476.4(8) Å^3, Z = 1, R = 0.0472, R_w^2 = 0.1166) strongly supports this hypothesis, since in the $[Zn_2\mathbf{L1}(\mu\text{-}PP)_2(MeOH)_2]^{2+}$ cation the diphosphate anions bridge the two metals. The dinuclear Zn(II) complexes of **L1** provide a simple model system for hydrolytic dizinc enzymes.

Introduction

Many enzymes, including those that hydrolyze phosphate esters, use two metal ions in a bifunctional catalytic mechanism.[1] Hydrolytic enzymes, such as alkaline phosphatases[2] and phospholipase C,[3] as well as the Klenow fragment of DNA polymerase I,[4] which is responsible for hydrolytic cleavage of the phosphodiester backbone of DNA, contain two metals in their active sites. The metal ions are often Zn(II). The catalytic role of zinc is ascribed to the binding and activation of substrates; a bridging coordination of the phosphate group gives a fundamental contribution to substrate activation. Furthermore, deprotonation of the Zn(II)-coordinated water to produce a nucleophilic zinc hydroxide is proposed as an essential catalytic function.

Synthetic metal complexes can be used as simple model systems for such enzymes. To this purpose, several mononuclear Zn(II) complexes have been studied in order to analyze binding and activation of phosphate esters.[5−9] Although dinuclear complexes have been also used in model studies on hydrolysis of phosphate esters, most of these have been accomplished with metals such as Cu(II), Co(III), or La(III).[10−12] Dinuclear synthetic Zn(II) complexes able to hydrolyze phos-

[†] University of Florence.
[‡] University of Urbino.
[⊗] Abstract published in *Advance ACS Abstracts,* May 15, 1997.

(1) (a) *Zinc Enzymes*; Bertini, I., Luchinat, C., Marek, W., Zeppezauer, M., Eds.; Birkauser: Boston, MA, 1986. (b) Kim, E. E.; Wyckoff, H. W. *J. Mol. Biol.* **1991**, *218*, 449−464. (c) Coleman, J. E. *Annu. Rev. Biophys. Biomol. Struct.* **1992**, *21*, 441−483. (d) Lipscomb, W. N.; Sträter, N. *Chem. Rev.* **1996,** *96*, 2375−2434. (e) Wilcox, D. E. *Chem. Rev.* **1996,** *96*, 2435−2458. (f) Steinhagen, H.; Helmchem, G. *Angew. Chem., Int. Ed. Engl.* **1996,** *35*, 2339−2342. (g) Sträter, N.; Lipscomb, W. N.; Klabunde, T.; Krebs, B. *Angew. Chem., Int. Ed. Engl.* **1996,** *35*, 2024−2055.
(2) (a) Gettins, P.; Coleman, J. E. *J. Biol. Chem.* **1994**, *259*, 4991−4997. (b) Ma, L.; Tibbitts, T. T.; Kantrovitz, E. R. *Protein Sci.* **1995**, *4*, 1498−1506.
(3) Hough, E.; Hansen, L. K.; Birknes, B.; Jynge, K.; Hansen, S.; Hardvik, A.; Little, C.; Dodson, E.; Derewenda, Z. *Nature* **1989**, *338*, 357−358.
(4) Beese, L. S.; Steiz, T. A. *EMBO J.* **1991**, *10*, 25−33.
(5) Gellman, S. H.; Petter, R.; Breslow, R. *J. Am. Chem. Soc.* **1986**, *108*, 2388−2394.
(6) (a) Koike, T.; Kimura, E. *J. Am. Chem. Soc.* **1991**, *113*, 8935−8941. (b) Koike, T.; Kimura, E.; Nakamura, I.; Hashimoto, Y.; Shiro, M. *J. Am. Chem. Soc.* **1992**, *114*, 7338−7345. (c) Kimura, E. *Tetrahedron* **1992**, *30*, 6175−6217. (d) Kimura, E.; Nakamura, I.; Koike, T.; Shionoya, M.; Kodama, Y.; Ikeda, T.; Shiro, M. *J. Am. Chem. Soc.* **1994**, *116*, 4764−4771. (e) Koike, T.; Kajitani, S.; Nakamura, I.; Kimura, E.; Shiro, M. *J. Am. Chem. Soc.* **1995**, *117*, 1210−1219. (f) Koike, T.; Kimura, E.; Kodama, M.; Shiro, M. *J. Am. Chem. Soc.* **1995**, *117*, 8304−8311.
(7) (a) Looney, A.; Parkin, G.; Alsfasser, R.; Ruf, M.; Vahrenkamp, H. *Angew. Chem., Int. Ed. Engl.* **1992**, *31*, 92−93. (b) Alsfasser, R.; Ruf, M.; Trofimenko, S.; Vahrenkamp, H. *Chem. Ber.* **1993**, *126*, 703−710. (c) Ruf, M.; Weis, K.; Vahrenkamp, H. *J. Chem. Soc., Chem. Commun.* **1994**, 135−136.
(8) Hikichi, S.; Tanaka, M.; Moro-oka, Y.; Kitajima, N. *J. Chem. Soc., Chem. Commun.* **1992**, 814−815.
(9) Garcia-España, E.; Luis, S. *Supramol. Chem.* **1996**, *6*, 257−266.
(10) (a) Chung, Y. S.; Akkaya, E. A.; Venkatachalam, T. K.; Czarnik, A. W. *Tetrahedron Lett.* **1990**, *31*, 5413−5416. (b) Vance, D. H.; Czarnik, A. W. *J. Am. Chem. Soc.* **1993**, *115*, 12165−12166.
(11) (a) Wall, M.; Hynes, R. C.; Chin, J. *Angew. Chem., Int. Ed. Engl.* **1993,** *32*, 1633−1634. (b) Takasaki, B. K.; Chin, J. *J. Am. Chem. Soc.* **1993**, *115*, 9337−9338. (c) Takasaki, B. K.; Chin, J. *J. Am. Chem. Soc.* **1994**, *116*, 1121−1122. (d) Connolly, J. A.; Banaszczyk, M.; Hynes, R. C.; Chin, J. *Inorg. Chem.* **1994**, *33*, 665−669. (e) Takasaki, B. K.; Chin, J. *J. Am. Chem. Soc.* **1995**, *117*, 8582−8585. (f) Wahnon, D.; Lebuis, A. M.; Chin, J. *Angew. Chem., Int. Ed. Engl.* **1995,** *34*, 2412−2414.
(12) Jones, D. R.; Lindoy, L. F.; Sargeson, A. M.; Snow, M. R. *Inorg. Chem.* **1982**, *21*, 4155−4160.

S0020-1669(96)01521-2 CCC: $14.00

Table 1. Crystal Data and Structure Refinement for $[Zn_2\mathbf{L1}(\mu\text{-PP})_2(MeOH)_2](ClO_4)_2$ PP^- = Diphenyl Phosphate)

empirical formula	$C_{46}H_{74}Cl_2N_6O_{22}P_2Zn_2$
formula weight	1326.70
temperature, K	293
wavelength, Å	0.71069
crystal system	triclinic
space group	$P\bar{1}$
unit cell dimensions	a = 10.681(5) Å, b = 12.042(1) Å, c = 13.191(3) Å, α = 74.63(2)°, β = 71.74(3)°, γ = 68.41(2)°
volume, Å^3	1476.4(8)
Z	1
density (calculated)	1.492 mg/m^3
absorption coefficient	1.037 mm^{-1}
crystal size	0.03 × 0.05 × 0.2 mm
reflections collected	4832
unique obs reflections [$I > 2\sigma(I)$]	3151
refined parameters	370
a, b	0.0676, 0.00
R[a] [$I > 2\sigma(I)$]	0.0472
$R_w{}^2$ [b]	0.1166

[a] $R = ||F_o| - |F_c||/|F_o|$. [b] $Rw^2 = [\sum w(F_o^2 - F_c^2)^2/\sum wF_o^4]^{1/2}$.

phate esters are rare. Recently, Kimura and co-workers have reported a dinuclear Zn(II) complex with a propanol-bridged octaazacryptand able to selectively recognize and hydrolyze phosphate monoesters.[13] Dimeric complexes with triaza macrocyclic units linked by different spacers have been studied by Breslow and co-workers as catalyst for hydrolysis of activated esters.[14]

Recently we have analyzed the coordination features of the macrocycle [30]aneN_6O_4 (**L1**) toward metal cations.[15] This ligand is composed of two triamine moieties linked by two dioxa chains and gives dinuclear Zn(II) complexes in aqueous solution; in these complexes each metal ion is coordinated by one triamine subunit, while the oxygens are weakly involved in metal coordination. The $[Zn_2[30]aneN_6O_4]^{4+}$ complex shows an unsaturated coordination sphere for the metals and gives dinuclear mono- and dihydroxo complexes in aqueous solution. These complexes are therefore promising model systems for hydrolytic dizinc enzymes.

In this paper we report on the ability of the dinuclear Zn(II) hydroxo complexes of [30]aneN_6O_4 to promote hydrolysis of activated carboxy and phosphate esters. The behavior toward activated esters of the Zn(II) complexes of the ligand [15]-aneN_3O_2 (**L2**) has been also studied. This latter can be considered as "half" **L1** and gives mononuclear **L2**−Zn and **L2**−Zn-OH complexes in aqueous solution.[16] The comparison between the activity of the dinuclear **L1** complexes and the mononuclear **L2** complexes can get insight into the role played by the presence of two coordinated Zn(II) ions at close distance within the same macrocyclic framework.

The crystal structure of the $[Zn_2\mathbf{L1}(\mu\text{-PP})_2(MeOH)_2](ClO_4)_2$ (**L1** = [30]aneN_6O_4, PP^- = diphenyl phosphate) adds further information on the interaction between phosphate esters and our dizinc complex.

Experimental Part

General Methods. UV spectra were recorded on a Shimadzu UV-2101PC spectrophotometer. ^{31}P NMR spectra (81.01 MHz) were recorded at 298 K in a Bruker AC-200 spectrometer. Peak positions

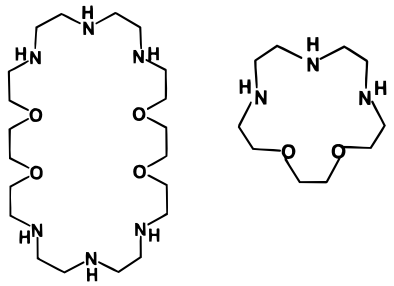

are reported relative to an external reference of 85% H_3PO_4. ^{31}P NMR titrations were performed by adding a MeOD solution of diphenyl hydrogen phosphate (1×10^{-2} M) and NaOD (1×10^{-2} M) to a solution of $[Zn_2\mathbf{L1}](ClO_4)_2\cdot 2H_2O$ (1×10^{-2} M) in MeOD.

All reagents and solvents used were of analytical grade. 4-Nitrophenyl acetate was recrystallized from diethyl ether.

Synthesis of the Compounds. 1,4,7,16,19,22-Hexaza-10,13,25,28-tetraoxacyclotriacontane (**L1**) and 1,4-dioxa-7,10,13-triazacyclopentadecane (**L2**) were prepared as previously described.[15,16]

$[Zn_2L1](ClO_4)_2\cdot 2H_2O$ (1). A sample of $Zn(ClO_4)_2\cdot 6H_2O$ (37.3 mg, 0.1 mmol) was added to an aqueous solution of $\mathbf{L1}\cdot 4.5HClO_4$ (44 mg, 0.05 mmol). $NaClO_4$ (100 mg) was added to the solution, and the pH was adjusted to 6 by addition of NaOH. By slow evaporation of the solution, a colorless powder crystallized, which was filtered, washed with ethanol, and dried in vacuum. Yield: 35 mg (87%). Anal. Calcd for $C_{20}H_{50}Cl_2N_6O_{14}Zn_2$: C, 30.15; H, 6.33; N, 10.55. Found: C, 30.2; H, 6.4; N, 10.5.

$[Zn_2L1(\mu\text{-PP})_2(MeOH)_2](ClO_4)_2$ (2). A sample of diphenyl hydrogen phosphate, HPP (5 mg, 0.02 mmol), was added to a methanolic solution (10 cm^3) of $[Zn_2\mathbf{L1}](ClO_4)_2\cdot 2H_2O$ (8.8 mg, 0.01 mmol). To the resulting solution was added 2 cm^3 of a 0.01 M NaOH methanolic solution. The solution was stirred at room temperature for 30 min and evaporated to 3 cm^3. Addition of butanol (10 cm^3) led to crystallization of compound **2**. Yield: 10.6 mg (80%). Anal. Calcd for $C_{46}H_{74}Cl_2N_6O_{22}P_2Zn_2$: C, 41.64; H, 5.62; N, 6.33. Found: C, 41.5; H, 5.6; N, 6.3.

Crystals suitable for X-ray analysis were obtained by slow evaporation of a methanol/butanol solution of **2**.

Caution! Perchlorate salts are potentially explosive; these compounds must be handled with great caution.

X-ray Structure Analysis. Analysis on a prismatic colorless single crystal of $[Zn_2\mathbf{L1}(\mu\text{-PP})_2(MeOH)_2](ClO_4)_2$ (**L1** = [30]aneN_6O_4, PP^- = diphenyl phosphate) was carried out with an Enraf-Nonius CAD4 X-ray diffractometer which uses an equatorial geometry, with graphite monochromated Mo Kα radiation. A summary of the crystallographic data is reported in Table 1.

Cell parameters for all compounds were determined by least-squares refinement of diffractometer setting angles for 25 carefully centered

(13) Koike, T.; Inoue, M.; Kimura, E.; Shiro, M. *J. Am. Chem. Soc.* **1996**, *118*, 3091−3099.
(14) Chapman, W. H., Jr.; Breslow, R. *J. Am. Chem. Soc.* **1995**, *117*, 5462−5469.
(15) Bazzicalupi, C.; Bencini, A.; Bianchi, A.; Fusi, V.; Paoletti, P.; Piccardi, G.; Valtancoli, B. *Inorg. Chem.* **1995**, *34*, 5622−5631.
(16) (a) Bazzicalupi, C.; Bencini, A.; Bianchi, A.; Fusi, V.; Paoletti, P.; Valtancoli, B. *J. Chem. Soc, Chem. Commun.* **1995**, 1555−1556. (b) Bazzicalupi, C.; Bencini, A.; Bianchi, A.; Corana, F.; Fusi, V.; Paoletti, P.; Paoli, P.; Valtancoli, B. *Inorg. Chem.* **1996**, *35*, 5540−5548.

reflections. Crystals of this compound belong to the triclinic family, space group $P\bar{1}$ ($Z = 1$), lattice constants $a = 10.681(5)$, $b = 12.042(1)$, and $c = 13.191(3)$ Å, $\alpha = 74.63(2)°$, $\beta = 71.74(3)°$, $\gamma = 68.41(2)°$, $V = 1476.4(8)$ Å^3.

The intensities of two standard reflections were monitored during data collections to check the stability of the diffractometer and of the crystal; no loss of intensity was recognized.

A total of 4832 reflections, up to $2\theta = 48°$ were collected. Intensity data were corrected for Lorentz and polarization effects, and an absorption correction was applied once the structure was solved by the Walker and Stuart method.[17]

The structure was solved by the heavy atom technique, which showed the metal center. Remaining non-hydrogen atoms were found by means of subsequent Fourier maps. Refinements were performed by means of the full-matrix least-squares method of SHELXL-93[18] program which uses the analytical approximation for the atomic scattering factors and anomalous dispersion corrections for all atoms from ref 19. The function minimized was $\sum w(F_o^2 - F_c^2)^2$ with $w = 1/[\sigma^2(F_o^2) + (aP)^2 + bP]$ and $P = (F_o^2 + 2F_c^2)/3$, where a and b are adjustable parameters (their final values are reported in Table 1).

All of the non-hydrogen atoms were refined using anisotropic displacement parameters. The hydrogen of the methanol molecule H31 was localized in the electronic density map, introduced in the calculation and isotropically refined. The remaining hydrogen atoms were introduced in calculated positions and their coordinates were refined in agreement with those of the linked atoms, with an overall thermal parameter refined up to a final value of 0.050(3) Å^2 for the hydrogens of the ethylenic and aromatic moieties, 0.048(8) Å^2 for hydrogens of the amine groups and 0.15(2) Å^2 for the hydrogens of methyl groups of the methanol molecules. For 370 refined parameters the final agreement factors were $R = 0.0472$ (for 3151 observed reflections with $I > 2\sigma(I)$) and $R_w^2 = 0.12$.

EMF Measurements. All potentiometric measurements (pH $= -\log[H^+]$) were carried out at 308.1 ± 0.1 K, by using the equipment which has been already described.[20] The reference electrode was an Ag/AgCl electrode in saturated KCl solution. The glass electrode was calibrated as a hydrogen concentration probe by titrating known amounts of HCl with CO_2-free NaOH solutions and determining the equivalent point by the Gran's method[21] which allows one to determine the standard potential $E°$, and the ionic product of water ($K_w = [H^+][OH^-]$). Titrations for the determination of the ligand basicity constants and Zn(II) complexation constants at 308.1 K were performed, in the pH range 2.5−10, by using CO_2-free aqueous solutions containing the metal ion and/or **L1** in 10^{-3} mol dm^{-3} concentrations. The system Zn−**L1** was studied both in 0.15 mol dm^{-3} NaCl and in 0.1 mol dm^{-3} NMe_4NO_3 at 308.1 K (NMe_4NO_3, p$K_w = 13.40$; NaCl, p$K_w = 13.36$). In order to evaluate the interaction of Cl^- and BNP with the Zn−**L1** complexes, titrations were performed in the presence of NaCl or BNP up to 30:1 Cl^-:Zn(II) and BNP:Zn(II) molar ratios in 0.1 mol dm^{-3} $NMe_4NO_3ClO_4$. The protonation constant of BNP was determined by separated measurements. The values obtained are equal within the experimental error to those already reported.[6a] No interaction with BNP was found in aqueous solution.

At least three measurements were performed for each system (100 data points each measurement). The computer program SUPERQUAD[22] was used to calculate both protonation and stability constants from emf data. The titration curves for each system were treated either as a single set or as independent entities without significant variations in the values of the stability constants.

Kinetics of *p*-Nitrophenyl Acetate Hydrolysis. The hydrolysis rate of 4-nitrophenyl acetate in the presence of the Zn−**L1** complexes was measured by an initial slope method following the increase in the 403 nm absorption of the released 4-nitrophenolate at 298.1 ± 0.1 K by using the procedure reported in ref 16b. The ionic strength was adjusted to 0.15 with NaCl. The reaction solution was maintained at 298.1 ± 0.1 K. MOPS (pH 7−7.8), TAPS (pH 7.8−8.9), and CHES (pH 8.9−9.5) buffers were used (50 mM). In a typical experiment, after 4-nitrophenyl acetate and $[Zn_2\mathbf{L1}](ClO_4)_2 \cdot 2H_2O$ (0.1−1 mM) in 10% CH_3CN solution at appropriate pH (the reference experiment does not contain the Zn(II) complex) were mixed, the UV absorption decay was recorded immediately and was followed generally until 2% decay of 4-nitrophenyl acetate. Two species, $[Zn_2\mathbf{L1}OH]^{3+}$ and $[Zn_2\mathbf{L1}(OH)_2]^{2+}$, promote NA hydrolysis; measurements in the pH range 6−7.8, where the $[Zn_2\mathbf{L1}(OH)_2]^{2+}$complex is absent from the solution, allow one to determine second-order k_{OH} constants for promoted hydrolysis by the monohydroxo species $[Zn_2\mathbf{L1}OH]^{3+}$ and to extrapolate the k_{OH} values for this species in the pH range 8−10, where both species are present in solution. Measurements in the pH range 8−10 lead to the determination of k_{OBS} values. The second-order rate constants $k_{(OH)2}$ for the dihydroxo complex $[Zn_2\mathbf{L1}(OH)_2]^{2+}$ are calculated by subtracting from the k_{OBS} value at a given pH the k_{OH} value at the same pH. Errors on k_{NA} values were about 10%.

Kinetics of Bis(*p*-nitrophenyl) Phosphate Hydrolysis. The hydrolysis rate of bis(*p*-nitrophenyl) phosphate to give mono(*p*-nitrophenyl) phosphate and *p*-nitrophenolate was measured by an initial slope method following the increase in the 403 nm absorption of the released *p*-nitrophenolate in aqueous solution at 308 ± 0.1 K. MOPS (pH 7−7.8), TAPS (pH 7.8−8.9), and CHES (pH 8.9−9.5) buffers were used (50 mM). The ionic strength was adjusted to 0.15 with NaCl. In a typical experiment, after bis(*p*-nitrophenyl) phosphate (1−10 mM) and $[Zn\mathbf{L2}](ClO_4)_2$ or $[Zn_2\mathbf{L1}](ClO_4)_4 \cdot 2H_2O$ (1−10 mM) aqueous solutions at appropriate pH (the reference experiment does not contain the Zn(II) complex) were mixed, the visible absorption increase was recorded immediately and was followed generally until 2% formation of *p*-nitrophenolate. A plot of the hydrolysis rate vs BNP^- concentration (1−10 mM) at a given pH gave a straight line, and then we determined the slope/[zinc complex] as the second-order rate constants k_{BNP} (M^{-1} s^{-1}). Errors on k_{BNP} values were about 5%.

Results and Discussion

Synthesis of $[Zn_2L1(\mu\text{-PP})_2(MeOH)_2](ClO_4)_2$. The reactivity toward substrate's molecules by dizinc complexes has been subject of a great deal of interest, due to their ability to reproduce the bimetallic structure presented by the active centers of several enzymes. A principal problem connected with low molecular weight dizinc model system for dizinc enzymes resides in the fact that their structures are often composed of two zinc(II) complex subunits kept together by bridging ligands and reaction with substrate's molecules can cleave the cluster and separate the metal centers. Such a problem has been nicely resolved by Lippard and co-workers, by using *m*-xylenediamine bis(Kemp's triacid imide) as efficient bridging ligand. This bridging dianion gives rise to a robust dizinc assembly.[23] As a different approach, two metal ions can be coordinated within the same macrocyclic framework, giving rise to a bimetallic core "protected" from cleavage upon reaction with substrate molecules.[24] The ligand **L1** binds two zinc ions both in aqueous and in methanolic solutions. From these solutions can be isolated solid $[Zn_2\mathbf{L1}](ClO_4)_4 \cdot 2H_2O$ (**1**), where two metals are enclosed within the macrocyclic cavity. Reaction of this complex with diphenyl phosphate was followed by means of ^{31}P NMR spectra recorded on methanolic solution containing **1** (1×10^{-2} M) and diphenyl

(17) Walker, N.; Stuart, D. D. *Acta Crystallogr., Sect. A* **1983**, *39*, 158−166.
(18) SHELXL-93: Sheldrick, G. M. *SHELXL-93*; University of Göttingen, Göttingen, Germany, 1993.
(19) *International Tables for X-ray Crystallography*; Kynoch: Birmingham, England, 1974; Vol. IV.
(20) Bianchi, A.; Bologni, L.; Dapporto, P.; Micheloni, M.; Paoletti, P. *Inorg. Chem.* **1984**, *23*, 1201−1205.
(21) (a) Gran, G. *Analyst* (*London*) **1952**, *77*, 661−663. (b) Rossotti, F. J.; Rossotti, H. *J. Chem. Ed.* **1965**, *42*, 375−378.
(22) Gans, P.; Sabatini, A.; Vacca, A. *J. Chem. Soc., Dalton Trans.* **1985**, 1195−1200.
(23) (a) Tanase, T.; Watton, S. P.; Lippard, S. J. *J. Am. Chem. Soc.* **1994**, *116*, 9401−9402. (b) Tanase, T.; Yun, J. W.; Lippard, S. J. *Inorg. Chem.* **1995**, *34*, 4220−4229. (c) Tanase, T.; Yun, J. W.; Lippard, S. J. *Inorg. Chem.* **1996**, *35*, 3585−3594 (d) Yun, J. W.; Tanase, T.; Lippard, S. J. *Inorg. Chem.* **1996**, *35*, 7590−7600.
(24) (a) Bazzicalupi, C.; Bencini, A.; Bianchi, A.; Fusi, V.; Paoletti, P.; Valtancoli, B. *J. Chem. Soc., Chem. Commun.* **1994**, 881−882. (b) Bazzicalupi, C.; Bencini, A.; Bianchi, A.; Fusi, V.; Mazzanti, L.; Paoletti, P.; Valtancoli, B. *Inorg. Chem.* **1995**, *34*, 3003−3010.

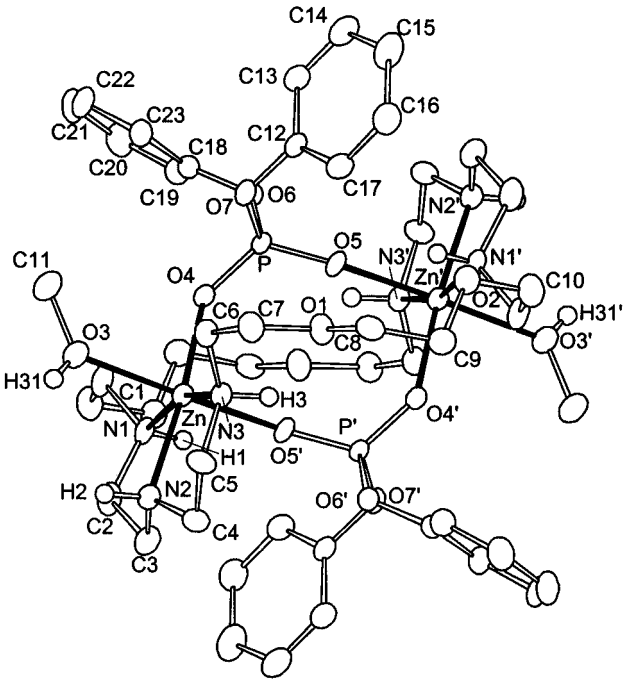

Figure 1. ORTEP drawing of the $[Zn_2\mathbf{L1}(PP)_2(MeOH)_2]^{2+}$ cation (PP^- = diphenyl phosphate).

phosphate (PP^-) in various molar ratios. Solutions containing **1** and increasing amounts of diphenyl phosphate, up to 1:1 molar ratio, shows one signal shifted upfield 4.56 ppm with respect to the "free" ester (Figure S1, Supporting Information). By adding further diphenyl phosphate, the signal shifts downfield. A linear correlation between the chemical shift and the **1**:PP^- ratio is found up to 1:2 molar ratio (in this condition the signal is shifted 3.41 ppm with respect to free PP^-). These results clearly account for the formation of a stable 1:1 complex in methanol between **1** and the phosphate ester at **1**: PP^- molar ratios greater than 1. Formation of a 1:2 complex takes place in the presence of an excess of diphenyl phosphate. The rather large shifts observed for the signal of phosphate bound to the bimetallic complex may indicate a bridging coordination of the phosphate anion. Indeed, solid $[Zn_2\mathbf{L1}(\mu\text{-}PP)_2(MeOH)_2](ClO_4)_2$ complex, where two PP^- anions bridge the metals, can be isolated in good yield from a methanolic solution containing **1** and PP^- in 1:2 molar ratio.

Description of the Structure of $[Zn_2L1(\mu\text{-}PP)_2(MeOH)_2](ClO_4)_2$. The crystal structure consists of $[Zn_2\mathbf{L1}(\mu\text{-}PP)_2(MeOH)_2]^{2+}$ (PP^- = diphenyl phosphate) cations and perchlorate anion. Each complex cation lies around a crystallographic center. Figure 1 shows an ORTEP[25] drawing of $[Zn_2\mathbf{L1}(\mu\text{-}PP)_2(MeOH)_2]^{2+}$ and Table 2 reports selected angles and distances.

Each metal center is hexacoordinated by the three nitrogens (N1, N2, and N3) of a triamine moiety, two oxygens (O4 and O5′) of two different phosphate esters, and an oxygen of a methanol molecule (O3). The geometrical arrangement of the donor atoms around each zinc atom results in a slightly distorted octahedron.

The two PP^- anions bridge the metal centers which lie 5.354(1) Å apart from each other. The five-membered ring formed by the bridging phosphate ester and the two zinc atoms has a twisted conformation, with a O4−Zn−Zn′−O5 torsional angle of 22.4°. The intraring O4−P−O5 angle has been expanded by *ca.* 13° from the ideal tetrahedral value to 122.3(2)°. A similar expansion has been already found by Lippard and co-workers in the crystal structure of the complex $[Zn_2(\mu\text{-XDK})(\mu\text{-PP})(PP)(CH_3OH)_2(H_2O)]$, where a diphenyl phosphate and an XDK (where H_2XDK is *m*-xylenediamine bis(Kemp's triacid imide)) anions bridge the two metal centers.[23c] While in the Lippard's complex the bridging XDK anion keeps the metals at close distance (3.846 Å), in our $[Zn_2\mathbf{L1}(\mu\text{-}PP)_2(MeOH)_2]^{2+}$ complex the flexibility of the macrocycle allows the two metal centers to lie at a larger distance (5.354 Å).

Table 2. Selected Distances (Å) and Angles (deg) for $[Zn_2\mathbf{L1}(\mu\text{-}PP)_2(MeOH)_2](ClO_4)_2$[a]

Zn−O4	2.007(3)	Zn−O3	2.254(4)
Zn−N2	2.131(3)	P−O4	1.480(3)
Zn−N1	2.136(3)	P−O5	1.475(3)
Zn−N3	2.162(3)	Zn−Zn′	5.354(1)
Zn−O5′	2.163(3)		
O4−Zn−N2	174.1(1)	O4−Zn−O3	85.8(1)
O4−Zn−N1	97.8(1)	N2−Zn−O3	88.4(1)
N2−Zn−N1	81.5(1)	N1−Zn−O3	92.5(1)
O4−Zn−N3	100.3(1)	N3−Zn−O3	93.1(1)
N2−Zn−N3	80.9(1)	O5′−Zn−O3	176.3(1)
N1−Zn−N3	161.4(1)	O4−P−O5	122.3(2)
O4−Zn−O5′	91.1(1)	P−O4−Zn	142.4(2)
N2−Zn−O5′	94.6(1)	P−O5−Zn′	161.3(2)
N1−Zn−O5′	85.9(1)	O4−Zn−Zn′	55.1
N3−Zn−O5′	89.4(1)	O5−Zn′−Zn	38.2

[a] Symmetry transformation used to generate equivalent atoms: (′) $-x, -y, -z$.

Enzymes able to cleavage phosphate ester bonds often contain carboxylate-bridged dimetallic cores, with consequent short intermetallic separations, as in the Klenow fragment of DNA polymerase I (3.9 Å).[4] A similar distance has been also found in alkaline phosphatase: a recent crystal structure of native *Escherichia coli* alkaline phosphatase complexed with inorganic phosphate shows the phoshate anion bridging the two Zn(II) ions, which lie 3.94 Å apart from each other.[2] Due to the flexibility of the macrocycle, in our dinuclear complex the Zn···Zn distance seems to be related to the characteristics of the bridging substrate. Recently, we reported the crystal structure of the $[Zn_2(\mu\text{-OH})\mathbf{L1}](ClO_4)_3$ complex.[15] The comparison between the conformation of the macrocycle in $[Zn_2(\mu\text{-OH})\mathbf{L1}]^{3+}$ and in the present $[Zn_2\mathbf{L1}(\mu\text{-}PP)_2(MeOH)_2]^{2+}$ cation confirms the flexibility of the macrocyclic backbone. In $[Zn_2(\mu\text{-OH})\mathbf{L1}]^{3+}$ the bridging hydroxide anion forces the two metals at close distance (3.54 Å) and the macrocycle assumes an overall screw-shaped conformation. On the contrary, in $[Zn_2\mathbf{L1}(\mu\text{-}PP)_2(MeOH)_2]^{2+}$ the macrocyclic framework is chair-shaped and more elongated. It seems likely that the flexibility of the macrocycle allows the two Zn(II) ions to achieve an appropriate distance for binding of substrate molecules.

Although several complexes with phosphate units bridging two Zn(II) ions are known,[6e,13,23c,26] our complex is one of the first dinuclear zinc complex solely bridged with phosphate esters. Previously Kitajima et al.[8] reported the crystal structure of a dizinc complex in which two ZnL units (L = hydrotris(3,5-diisipropyl-1-pyrazolyl)borate) are solely bridged by a phosphate ester, with a Zn−Zn distance of 5.1 Å, similar to that found in our case.

Zn(II) Complexes Formation in Aqueous Solution. Table 3 collects the stability constants for the complexes of **L1** and **L2** with Zn(II), potentiometrically determined in 0.15 mol dm^{-3} NaCl aqueous solution at 308.1 K. In the case of **L1**, the

(25) Johnson, C. K. ORTEP. Report ORNL-3794; Oak Ridge National Laboratory: Oak Ridge, TN, 1971.

(26) (a) Orioli, P.; Cini, R.; Donati, D.; Mangani, S. *J. Am. Chem. Soc.* **1981**, *103*, 4446−4447. (b) Song, T.; Xu, J.; Zhao, Y.; Yue, Y.; Xu, Y.; Xu, R.; Hu, N.; Wei, G.; Jia, H. *J. Chem. Soc., Chem. Commun.* **1994**, 1171−1172 (c) Bissinger, P.; Kumberger, O.; Schier, A. *Chem. Ber.* **1991,** *124*, 509.

Table 3. Logarithms of the Equilibrium Constants for the Complexation Reactions of Zn^{2+} with **L1** and **L2**

	L1			
reaction	NaCl[a] (308.1 K)	Me_4NNO_3[b] (308.1 K)	NaCl[c] (298.1 K)	**L2** NaCl[a] (308.1 K)
$Zn^{2+} + \mathbf{L} = Zn\mathbf{L}^{2+}$	7.8(1)	8.0(1)	8.73	9.0(1)
$Zn\mathbf{L}^{2+} + H^+ = Zn\mathbf{L}H^{3+}$	8.4(1)	8.4(9)	8.4	
$Zn\mathbf{L}H^{3+} + H^+ = Zn\mathbf{L}H_2^{4+}$	7.2(1)	6.7(1)	7.17	
$Zn\mathbf{L}^{2+} + OH^- = Zn\mathbf{L}OH^+$			4.5	4.8(1)
$2Zn^{2+} + \mathbf{L} = Zn_2\mathbf{L}^{4+}$	13.7(1)	13.4(1)	14.2	
$Zn_2\mathbf{L}^{4+} + OH^- = Zn_2\mathbf{L}OH^{3+}$	6.1(1)	6.3(1)	6.1	
$Zn_2\mathbf{L}OH^{3+} + OH^- = Zn_2\mathbf{L}(OH)_2^{2+}$	4.1(1)	4.3(1)	4.5	

[a] This work, $I = 0.15$ M NaCl, 308.1 K, $pK_w = 13.40$. [b] This work, $I = 0.1$ M NMe_4NO_3, 308.1 K, $pK_w = 13.36$. [c] From ref 8, $I = 0.15$ M NaCl, 298.1 K, $pK_w = 13.73$.

stability constants have been also measured in 0.1 mol dm^{-3} NMe_4NO_3 aqueous solution at 308.1 K.[27] The stability constants are similar in both ionic media. In the case of **L2** a monohydroxo species **L2**−Zn-OH^+ is present in solution from neutral to alkaline pH, while the dinuclear Zn(II) complex of **L1** gives rise to a monohydroxo and a dihydroxo species. A distribution diagram for the system Zn/**L1** in 2:1 molar ratio at 308.1 K is provided in the Supporting Information (Figure S2). The most relevant difference between the Zn−**L1** system at 298.1 K[16] and at 308.1 K is the lower stability of the $[Zn\mathbf{L1}]^{2+}$ and $[Zn_2\mathbf{L1}]^{4+}$ at the higher temperature, due to the exothermicity of the process of metal coordination; on the contrary, the pK_a values of the coordinated water decrease at the higher temperature (for example, considering the formation of the $[Zn_2\mathbf{L1}OH]^{3+}$ species, pK_a values of 7.3 at 308.1 K and 7.6 at 298.1 K can be calculated from Table 3). This is likely due to the endothermicity of the process of acidic dissociation of coordinated water molecules. These two effects reduce the percentages of $[Zn\mathbf{L1}]^{2+}$ and $[Zn_2\mathbf{L1}]^{4+}$ formed at 308.1 K. The $[Zn\mathbf{L1}OH]^+$ species is even not detectable at this temperature.

Considering the binding of chloride, measurements carried out on the system Zn−**L1** in NMe_4NO_3 in the presence of increasing amount of NaCl allow us to evidence the formation of a $[Zn_2\mathbf{L1}Cl]^{3+}$ complex, which is present in solution at acidic pH. However, the rather low constant for the addition of Cl^- to the dinuclear complex (log $K = 1.6$ for the equilibrium $Zn_2\mathbf{L1}^{4+} + Cl^- = Zn_2\mathbf{L1}Cl^{3+}$) indicates a low affinity of the dinuclear complex for this halide. Therefore Cl^- is replaced by the strongly bound hydroxide ion since neutral pH. Even in the presence of a high concentration of chloride, the distribution curves of the monohydroxo $[Zn_2\mathbf{L1}OH]^{3+}$ and dihydroxo $[Zn_2\mathbf{L1}(OH)_2]^{2+}$ complexes do not significantly differ from those found in the absence of Cl^-.

4-Nitrophenyl Acetate Hydrolysis. Both dinuclear hydroxo complexes of the ligand **L1**, $[Zn_2\mathbf{L1}OH]^{3+}$ and $[Zn_2\mathbf{L1}(OH)_2]^{2+}$, promote NA hydrolysis, and second-order kinetics is followed at different pH values. In Figure 2 the k_{NA} values are reported as a function of the concentration of the hydroxo complexes $[Zn_2\mathbf{L1}OH]^{3+}$, $[Zn_2\mathbf{L1}(OH)_2]^{2+}$. The k_{NA} values for the monohydroxo Zn(II) complex with the ligand **L2**, **L2**−Zn-OH^+, are also reported. No effect is observed below pH 6, where such hydroxo species are absent in solutions. In all three cases, the plots give rise to straight lines.

These results indicate that the Zn−**L** (**L** = **L1** and **L2**) hydroxo complexes are the kinetically active species, *i.e.*, the Zn(II)−OH species is indeed a nucleophile. Furthermore, the hydrolysis of the ester occurs *via* a bimolecular mechanism, which would involve the nucleophilic attack of the metal-bound hydroxide to the carbonyl group of the ester and release of *p*-nitrophenate. The $[Zn_2\mathbf{L1}OH]^{3+}$, $[Zn_2\mathbf{L1}(OH)_2]^{2+}$, and **L2**−Zn-$OH^+$ are formed in 30−60% in the pH ranges used in the kinetic measurements (Figure S2 and Tables S1−S3, Supporting Information). As a consequence, in order to compare the activity of our complexes, second-order rate constants k'_{NA} have been determined from the maximum k_{NA} values by using the following equation:

$$v = k_{NA}[\text{total Zn(II)complex}][p\text{-nitrophenylacetate}] = k'_{NA}[Zn\mathbf{L}(OH)^+][p\text{-nitrophenyl acetate}]$$

The k'_{NA} values for our hydroxo complexes are reported in Table 4, together with the rate constants found for NA hydrolysis promoted by the hydroxo-Zn(II) complexes with 1,5,9-triazacyclododecane ([12]aneN$_3$−Zn-OH^+) and 1,4,7,10-tetraazacyclotetradecane ([14]aneN$_4$−Zn-OH^+).[6a] The corresponding pK_a

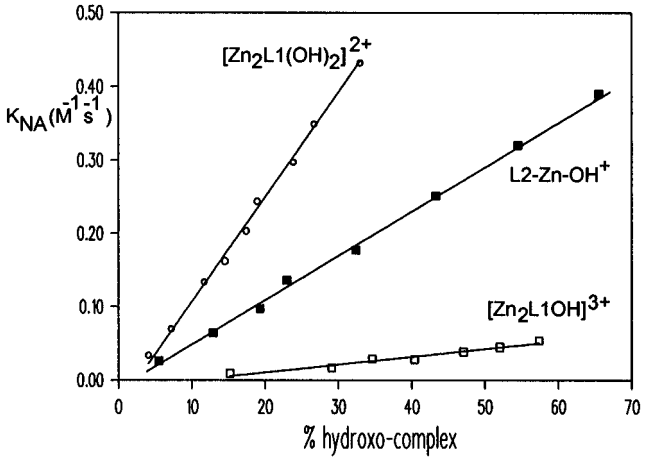

Figure 2. Second-order rate constants for NA hydrolysis (k_{NA}) as a function of the percentage of the hydroxo complexes $[Zn_2\mathbf{L1}(OH)]^{3+}$ (□), $[Zn_2\mathbf{L1}(OH)_2]^{2+}$ (○), and **L2**−Zn-OH (■), determined in 0.15 M NaCl aqueous solution at 308.1 K.

Table 4. Second-Order Rate Constants k'_{NA} (M^{-1} s^{-1}) for Hydrolysis of 4-Nitrophenyl Acetate at 298.1 K

nucleophile	k'_{NA}	$pK_a(H_2O)$
$[Zn_2\mathbf{L1}(OH)]^{3+}$ [a]	$(9.4 \pm 1) \times 10^{-2}$	7.6[c]
$[Zn_2\mathbf{L1}(OH)_2]^{2+}$ [a]	1.3 ± 0.1	9.2[d]
L2−Zn-OH^+ [a]	$(6.0 \pm 0.6) \times 10^{-1}$	8.8[e]
[12]aneN$_3$−Zn-OH^+ [b]	4.1×10^{-2}	7.2[e]
[14]aneN$_4$−Zn-OH^+ [b]	1.1×10^{-1}	7.9[e]

[a] $I = 0.15$ M NaCl. [b] From ref 6a, $I = 0.1$ M $NaClO_4$. [c] $K_a = [Zn_2\mathbf{L1}(OH)^{3+}][H^+]/[Zn_2\mathbf{L1}^{4+}]$. [d] $K_a = [Zn_2\mathbf{L1}(OH)_2^{2+}][H^+]/[Zn_2\mathbf{L1}(OH)^{3+}]$. [e] $K_a = [\mathbf{L}-Zn\text{-}OH^+][H^+]/[\mathbf{L}-Zn^{2+}]$ (**L** = **L2**, [12]aneN$_3$, or [14]aneN$_4$).

(27) Protonation constants of **L1** at 308.1 K: log $K_1 = 9.17(3)$, log $K_2 = 8.56(3)$, log $K_3 = 7.90(3)$, log $K_4 = 7.05(3)$, log $K_5 = 3.79(4)$, log $K_6 = 2.89(4)$ (0.15 mol dm^{-3} NaCl aqueous solution); log $K_1 = 9.51(3)$, log $K_2 = 8.52(3)$, log $K_3 = 7.95(4)$, log $K_4 = 7.19(4)$, log $K_5 = 3.93(6)$, log $K_6 = 3.06(6)$ (0.1 mol dm^{-3} NMe_4ClO_4 aqueous solution). Protonation constants of **L2** at 308.1 K: log $K_1 = 9.35(2)$, log $K_2 = 8.39(2)$, log $K_3 = 2.34(3)$ (0.15 mol dm^{-3} NaCl aqueous solution). $K_n = [\mathbf{L}H_n^{n+}]/[\mathbf{L}H_{(n-1)}^{(n-1)+}][H^+]$.

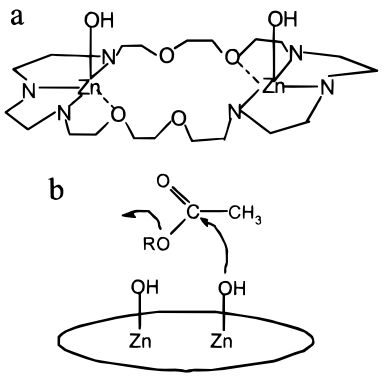

Figure 3. (a) Proposed structure for the $[Zn_2\mathbf{L1}(OH)_2]^{2+}$ cation. (b) Proposed mechanism for hydrolysis of NA by $[Zn_2\mathbf{L1}(OH)_2]^{2+}$.

values for dissociation of the coordinated water molecule are also reported. Table 4 clearly shows that the hydrolytic activity is related to the pK_a of the coordinated water molecule, *i.e.*, the complexes with higher pK_a give higher rate constants. These findings are in good accord with the simple nucleophilic mechanism proposed by Kimura and co-workers for hydrolysis of carboxylic ester.

Considering the dinuclear **L1** complexes, the monohydroxo $[Zn_2\mathbf{L1}OH]^{3+}$ complex shows a remarkably lower rate constant than the dihydroxo $[Zn_2\mathbf{L1}(OH)_2]^{2+}$ one (9.4×10^{-2} *vs* 1.3 M^{-1} s^{-1}). The dinuclear **L1** complex shows an undoubtedly low pK_a value (7.6 at 298.1 K) for the formation of the monohydroxo complex $[Zn_2\mathbf{L1}(OH)]^{3+}$. Such a high tendency to deprotonation of coordinated water molecule has been attributed to a bridging coordination of hydroxide to the two metals, as actually shown by the crystal structure of the $[Zn_2\mathbf{L1}(\mu\text{-OH})](ClO)_4$ salt.[15] In $[Zn_2\mathbf{L1}(\mu\text{-OH})]^{2+}$ the $[Zn_2(\mu\text{-OH})]$ unit is tightly encapsulated within the macrocyclic framework. The macrocycle assumes a screw-shaped conformation, defining a tridimensional internal cavity where the $[Zn_2(\mu\text{-OH})]$ unit is lodged. Each Zn(II) ion seems to be coordinately almost saturated and shielded, making the dizinc hydroxo function of low availability for the bimolecular hydrolytic process. The much higher activity of the dihydroxo $[Zn_2\mathbf{L1}(OH)_2]^{2+}$ species may be related to a more "opened" conformation of the macrocycle, which can leave catalytic sites accessible on the two Zn(II) ions. A proposed structure for this species is sketched in Figure 3a. Actually, as discussed above, the macrocyclic framework is rather flexible, allowing the two metal centers to modulate their separation in order to achieve an appropriate distance for the catalytic process.

Finally, comparing the activity of the complexes of **L1** and **L2,** it is to be noted that the dinuclear $[Zn_2\mathbf{L1}(OH)_2]^{2+}$ species is *ca*. twice more active than the mononuclear **L2**−Zn-OH^+ complex. This observation seems to indicate that the two metal centers do not play any cooperative role in NA hydrolysis. The 2-fold activity of the dinuclear complex could be speculatively attributed to the presence of two nucleophilic Zn-OH functions in $[Zn_2\mathbf{L1}(OH)_2]^{2+}$. However, it seems likely that a simple nucleophilic mechanism is predominant, and in both the mononuclear **L2** and in the dinuclear **L1** complexes a Zn-OH species acts merely as a nucleophile, as sketched in Figure 3b.

Bis(4-nitrophenyl) Phosphate Hydrolysis. The mononuclear **L2**−Zn-OH^+ and the dinuclear $[Zn_2\mathbf{L1}(OH)_2]^{2+}$ complexes promote bis(*p*-nitrophenyl) phosphate (BNP) hydrolysis in aqueous solution at 308.1 K to give mono(*p*-nitrophenyl) phosphate and *p*-nitrophenate. Second-order rate constants k_{BNP} have been determined at different pH values for both complexes. The mono(*p*-nitrophenyl) phosphate formed is not further hydrolyzed. In Figure 4 the k_{BNP} values for the Zn−**L1** and Zn−**L2** complexes are reported as a function of pH, together

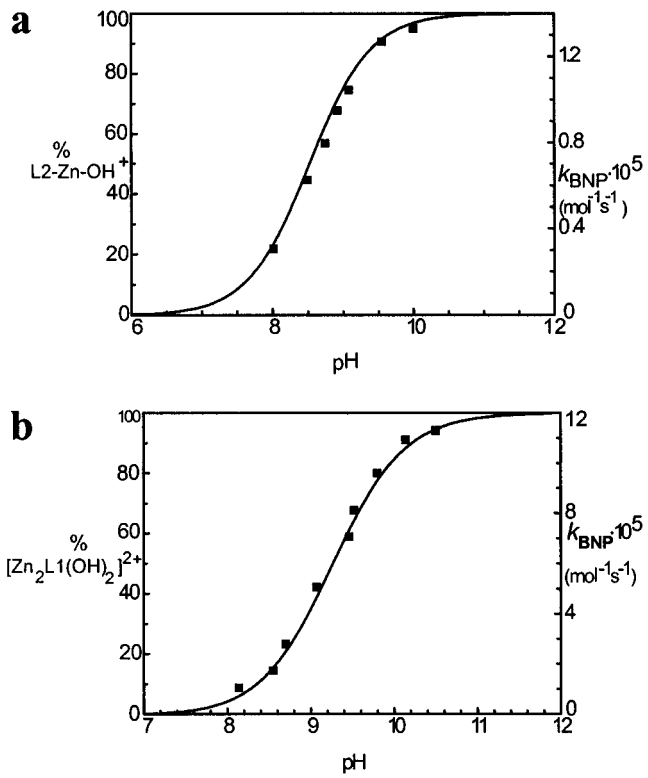

Figure 4. (a) Plot of the distribution curve of **L2**−Zn-OH^+ (solid line, left *Y* axis) and k_{BNP} values (■, right *Y* axis) as a function of pH (0.15 mol dm^{-3} NaCl, 308.1 K). (b) Plot of the distribution curve of $[Zn_2\mathbf{L1}(OH)_2]^{2+}$ (solid line, left *Y* axis) and k_{BNP} values (■, right *Y* axis) as a function of pH (0.15 mol dm^{-3} NaCl, 308.1 K).

Table 5. Second-Order Rate Constants k_{BNP} (M^{-1} s^{-1}) for Hydrolysis of Bis(4-nitrophenyl) Phosphate at 308.1 K

nucleophile	k_{BNP}
$[Zn_2\mathbf{L1}(OH)_2]^{3+}$ [a]	$(1.15 \pm 0.06) \times 10^{-4}$
L2−Zn-OH^+ [b]	$(1.31 \pm 0.07) \times 10^{-5}$
[12]aneN_3−Zn-OH^+ [c]	8.5×10^{-5}
[14]aneN_4−Zn-OH^+ [d]	2.1×10^{-5}

[a] $I = 0.15$ M NaCl, pH 10.5. [b] $I = 0.15$ M NaCl, pH 10. [c] From ref 6a, $I = 0.2$ M $NaClO_4$, pH = 8.6. [d] From ref 6a, $I = 0.2$ M $NaClO_4$, pH = 9.2.

with the distribution curve of the $[Zn_2\mathbf{L1}(OH)_2]^{2+}$ and **L2**−Zn-OH^+ species at 308.1 K. A good fitting between the k_{BNP} values and the distribution curve of the **L2**−Zn-OH^+ and of the $[Zn_2\mathbf{L1}(OH)_2]^{2+}$ species are found. Accordingly, it can be concluded that **L2**−Zn-OH^+ and $[Zn_2\mathbf{L1}(OH)_2]^{2+}$ are kinetically active species. On the contrary, the monohydroxo species $[Zn_2\mathbf{L1}(OH)]^{3+}$ does not promote this hydrolytic process, in accord with the very low activity in NA hydrolysis found for this species.

Table 5 reports the k_{BNP} values for the $[Zn_2\mathbf{L1}(OH)_2]^{2+}$ and **L2**−Zn-OH^+ complexes, together with the rate constants found for [12]aneN_3−Zn-OH^+ and [14]aneN_4−Zn-OH^+. Our mononuclear **L2**−Zn-OH^+ complex shows a lower activity than the Zn(II) complexes with [12]aneN_3 and [14]aneN_4. On the other hand, the rate constant for the dinuclear $[Zn_2\mathbf{L1}(OH)_2]^{2+}$ complex is higher than those found for the mononuclear ones. In particular, the dinuclear $[Zn_2\mathbf{L1}(OH)_2]^{2+}$ complex is almost 10 times more active than the mononuclear **L2**−Zn-OH^+ one. As above reported, such a remarkable difference in activity between the mononuclear **L2** complex and the dinuclear **L1** one is not observed in acetate hydrolysis. For BNP hydrolysis catalyzed by mononuclear Zn(II) complexes, Kimura and co-workers proposed a mechanism where the Zn(II)-OH function

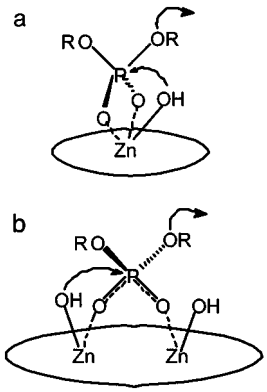

Figure 5. Proposed mechanisms for hydrolysis of BNP by **L2**−Zn-OH^+ (a) and by $[Zn_2\mathbf{L1}(OH)_2]^{2+}$ (b).

acts as nucleophile and at the same time Zn(II) offers an electrophilic binding site for P−O.[6c] Such a mechanism can be also assumed for BNP hydrolysis by our mononuclear **L2**−Zn-OH complex (Figure 5a). As far our dinuclear $[Zn_2\mathbf{L1}(OH)_2]^{2+}$ is concerned, the higher activity in BNP hydrolysis can be explained by considering that the phosphate ester interacts with two electrophilic Zn(II) centers (Figure 5b), and at same time one Zn-OH function operates the nucleophilic attack to phosphorus. In other words, in BNP hydrolysis promoted by the dinuclear $[Zn_2\mathbf{L1}(OH)_2]^{+}$ complex, the two Zn(II) ions play a cooperative role. A bridging interaction of the phosphate ester to the two metal ions in the hydrolytic mechanism can be suggested. Actually, the crystal structure of the $[Zn_2\mathbf{L1}(\mu\text{-PP})_2(MeOH)_2]^{2+}$ cation shows the phosphate unit bridging the two metals, strongly supporting our proposed mechanism.

Concluding Remarks. The mononuclear **L2**−Zn-OH^+ and the dinuclear $[Zn_2\mathbf{L1}(OH)_2]^{2+}$ complexes exhibit different rate enhancements in NA and BNP hydrolysis. In NA hydrolysis, a simple nucleophilic mechanism (Figure 3b) leads to a similar activity of the two complexes (the dinuclear complex is only twice more active than the mononuclear one), while in BNP hydrolysis interaction of phosphate ester with the two electrophilic centers of $[Zn_2\mathbf{L1}(OH)_2]^{2+}$ (Figure 5b) determines the much higher activity of the dinuclear $[Zn_2\mathbf{L1}(OH)_2]^{2+}$ complex with respect to the mononuclear **L2**−Zn-OH^+ one. The crystal structure of the $[Zn_2\mathbf{L1}(\mu\text{-PP})_2(MeOH)_2](ClO_4)_2$ complex (PP^- = diphenyl phosphate) supports this hypothesis. In the $[Zn_2\mathbf{L1}(\mu\text{-PP})_2(MeOH)_2]^{2+}$ cation the diphenyl phosphate anions bridge the two metal ions. The structural results, together with the kinetic data, suggest that the substrate approaches the $[Zn_2\mathbf{L1}(OH)_2]^{2+}$ complex and two oxygens of BNP start associating with the two Zn(II) ions of the complex. Simultaneously a Zn-OH function operates a nucleophilic attack on the phosphorus, followed by the cleavage of the phosphate ester bond.

The present dinuclear complex can provide useful model systems for hydrolytic dizinc enzymes, where a bridging coordination of phosphate units has been suggested to play a fundamental role in phosphate ester activation and hydrolysis.

Acknowledgment. Financial support by Italian Ministero dell'Università e della Ricerca Scientifica e Tecnologica (quota 40%) and CNR (Consiglio Nazionale delle Ricerche) is gratefully acknowledged.

Supporting Information Available: Plot of the ^{31}P chemical shifts of PP^- as a function of the [**1**]:PP^- molar ratio, distribution diagram for the system **L1**−Zn at 308.1 K, plot of the k_{BNP} values as a function of the percentage of **L2**−Zn-OH^+ and $[Zn_2\mathbf{L1}(OH)_2]^{2+}$, tables of k_{NA} and k_{BNP} values at different pH values, and tables of crystallographic and experimental data, complete atomic positional parameters, anisotropic temperature factors, and bond distances and angles for **2** (15 pages). Ordering information is given on any current masthead page.

IC961521J